

# COMBINED CYCLIC BENDING-TORSIONAL LOADING TEST OF REINFORCED CONCRETE BRIDGE COLUMNS

Paiboon Tirasit<sup>1</sup> and Kazuhiko Kawashima<sup>2</sup>

## Abstract

Torsion probably takes place in the piers of some specific bridges during an earthquake and affects the pier seismic performance. This paper presents an experimental study on the inelastic behavior of reinforced concrete columns under combined action of cyclic bending and torsional loading. Seven reinforced concrete columns were tested under three loading conditions: 1) cyclic uniaxial bending; 2) cyclic torsion; and 3) combined cyclic bending and cyclic torsion, with and without a constant axial compression force. A parameter called “rotation-drift ratio” ( $r$ ) was introduced to represent the level of combined cyclic bending and torsion. The experimental result indicates that the flexural capacity of reinforced concrete column decreases and the damage tends to occur above the flexural plastic hinge region as the rotation-drift ratio  $r$  increases.

## Introduction

Presently, because of the space limitation for the transportation system in many urban areas, bridges with particular configurations, such as C-bent column bridges, skewed bridges and curved bridges, are often used. Due to their irregular structural configurations, the special seismic consideration is required to design these bridges to be able to survive extreme ground motions. Since the center of mass of superstructure does not coincide with the center of rigidity in C-bent columns, torsion coupled with other internal forces can occur during an earthquake. In skewed bridges, the collision between bridge deck and abutments or adjacent spans possibly takes place during a ground excitation and it subsequently causes the deck rotation about the vertical axis (Watanabe et al. 2004). This may induce the twisting moment in the piers (Paiboon et al. 2005). Moreover, the responses of curved bridges in the transverse and longitudinal directions are coupled, and the piers are subsequently subjected to the multi-directional deformation with torsion. The combination of seismic torsion and other internal forces can result in the complex flexural and shear failure of these bridge piers.

Although there have been a number of researches about the effect of twisting moment on the behavior of reinforced concrete member, most of them have focused on the monotonic load test. However, Hsu et al. (2000) and Hsu et al. (2003) conducted the experimental studies on the effect of combined cyclic bending and constant torsion on the performance of composite columns with H steel sections and hollow composite columns. They found that the flexural capacity and ductility of composite columns decreased when a constant torsion was simultaneously applied. The effect of torsion on the deterioration of flexural strength was more considerable in the composite columns with larger aspect ratio. Kawashima et al. (2003) and Nagata et al. (2004) conducted a cyclic bilateral loading test and a hybrid loading test, respectively, on the reinforced

---

<sup>1</sup> Graduate Student, Dept. of Civil Engineering, Tokyo Institute of Technology

<sup>2</sup> Professor, Dept. of Civil Engineering, Tokyo Institute of Technology

concrete C-bent columns. They revealed that the damage occurred severely on the eccentric compression side and the residual displacement happened in this direction. This was resulted from the eccentricity of vertical axial load cooperated with the bending moment and torsion from the eccentric lateral force. Otsuka et al. (2003) carried out an experimental study on the performance of reinforced concrete columns under cyclic torsional loading. Their results indicated that the increase of axial force and amount of tie reinforcement enhanced the torsional capacity. Axial force and amount of tie bars affected the secondary stiffness of torsional hysteretic envelope. Otsuka et al. (2004) also conducted a cyclic loading test on the reinforced concrete columns by applying combined cyclic bending and torsion once at each loading step. They found that the spacing of tie reinforcement remarkably affected the torsional hysteretic loops but less significantly influenced on flexural hysteretic loops.

However, there exist many unknowns on the effect of combined action of cyclic bending and torsion on the performance of reinforced concrete columns. Furthermore, the reliable torsional hysteretic model for the response analysis has not yet been available.

This paper presents a series of cyclic loading test of reinforced concrete columns to investigate the effect of combined cyclic bending and torsional loading on the column behavior. The experimental results about the progress of column failure, damage patterns, hystereses and deformation of reinforcements are presented and discussed.

## Experimental Program

### Column Properties

Seven reinforced concrete columns were constructed with the same structural properties as shown in Fig. 1. The column cross section was 400 mm x 400 mm square. The column was 1750 mm tall with a 1350 mm effective height measured from the bottom of column to the loading point. The columns were designed based on the

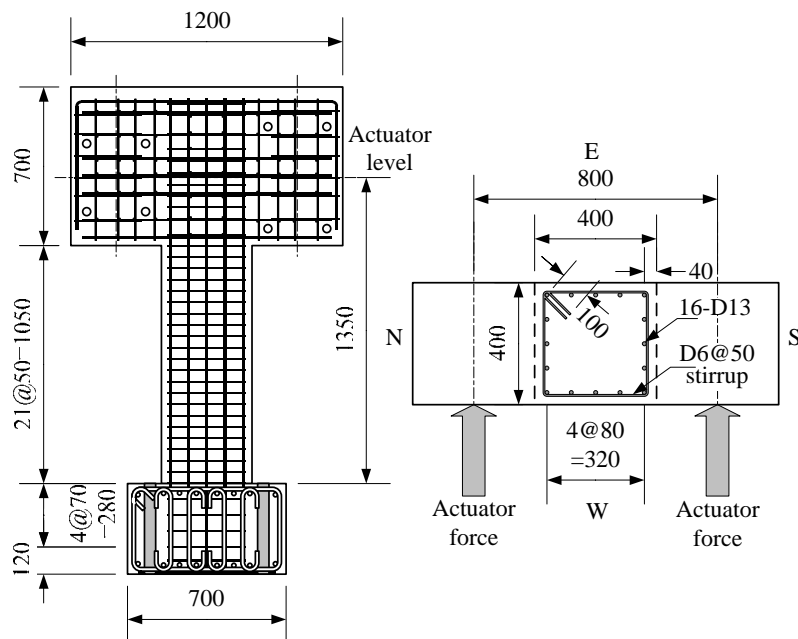


Fig. 1 Specimen configuration

Japanese 1996 Design Specification of Highway Bridges (Japan Road Association 1996). Type I (middle-field) and Type II (near-field) ground motions with the moderate soil condition were assumed. The axial compression stress at the flexural plastic hinge region of the columns due to the superstructure dead weight was assumed to be 1 MPa which is typical in Japanese bridge piers. Sixteen 13 mm diameter deformed bars with a 295 MPa nominal strength (SD295A) were employed as the longitudinal reinforcement. The same class 6 mm deformed bars were used as the tie reinforcement with 50 mm spacing along the column axis. The tie bars were anchored using 135 degree bent hooks with a development length of 100 mm. The yield strengths of longitudinal and tie reinforcements were 353.7 MPa and 328 MPa, respectively. The longitudinal reinforcement ratio and the tie volumetric ratio were 1.27% and 0.79%, respectively. The design compressive strength of concrete was 30 MPa. Table 1 shows the concrete strength  $f'_c$  obtained from the cylinder test. Because cylinder test was not conducted for P3 and P5, measured strength of concrete is not available. However, because the concrete was mixed and casted in the same way with other specimens, the concrete strength must be very similar with others. It is noted that these material properties and amount of reinforcements correspond to those of piers in typical bridges.

### ***Experimental Setup and Loading***

The cyclic loading test was conducted at the dynamic loading laboratory in Tokyo Institute of Technology. The experimental setup is shown in Fig. 2. The column was anchored to the test floor by using four PC bars with 250 kN prestressing force each. Table 1 shows the loading conditions of the columns. A constant 160 kN compression load was applied to the columns by the vertical actuator in order to produce a 1 MPa compressive stress at the flexural plastic hinge region. To apply cyclic uniaxial bending, cyclic torsion and combined cyclic uniaxial bending and torsion to the columns, lateral displacement and rotation were generated by controlling two horizontal actuators as shown in Fig. 2(b). Cyclic uniaxial bending was created by driving two horizontal actuators with the same displacement commands while cyclic torsion and combined cyclic uniaxial bending and torsion were generated by imposing different displacement commands in two actuators. It should be noted that because flexural displacement and rotation were imposed in phase, loading displacement from combined bending and torsion was always larger at horizontal actuator 1 than horizontal actuator 2. This results in more significant damage at S surface than N surface as will be discussed later.

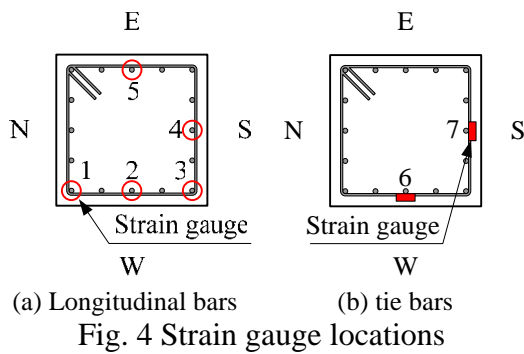
A non-dimensional parameter called “rotation-drift ratio”,  $r$ , is introduced here to define the level of combined cyclic bending and torsion as

$$r = \frac{\theta}{\Delta} \quad (1)$$

where  $\theta$  is the column rotation (radian) and  $\Delta$  is the lateral drift of column.

The rotation-drift ratios  $r$  and the applied lateral drifts and rotations of every loading step of all columns are presented in Table 2. P1 was tested under cyclic uniaxial bending. To investigate the effect of axial force on the torsional hysteresis of column, P2 and P3 were tested under pure cyclic torsion without and with an axial compression force, respectively. Results from P1 and P3 were used as the references of this study. P4 to P7 were loaded under several combinations of cyclic bending and torsion which were represented by the rotation-drift ratio  $r$  defined by Eq. (1). The lateral drift and





rotation were simultaneously applied three cycles at every loading step as shown in Fig. 3.

In order to study the deformation of reinforcements under different loading conditions, electronic strain gauges were attached to the surfaces of the longitudinal and tie reinforcements as shown in Fig. 4. In P2 and P3 which were subjected to pure cyclic torsion, the strain gauge was not provided at No.5. The

strain gauges on the longitudinal reinforcement of P2 and P3 were mounted at 25 mm, 275 mm, 525 mm and 775 mm from the base of column and the strain gauges on the tie reinforcement were placed at 50 mm, 250 mm, 500 mm and 750 mm from the bottom of column. However, the strain gauges were installed to the longitudinal reinforcement at 25 mm, 275 mm and 525 mm from the base of column and the strain gauges on the tie reinforcement were located at 50 mm, 150 mm, 250 mm, 350mm and 500 mm from the bottom of column in P1 which was subjected to cyclic uniaxial bending and P4 to P7 which were subjected to combined action of cyclic bending and cyclic torsion.

## Damage and Hystereses of Columns

### Column under Cyclic Uniaxial Bending

Fig. 5(a) presents the damage at the completion of loading at 5% drift of P1 which was subjected to cyclic uniaxial bending with the axial force. The covering concrete on E surface in the plastic hinge region firstly suffered the compression failure at 3% drift. Consequently, the spalling off began to take place in the covering concrete and the longitudinal and tie reinforcements were uncovered at 4% drift. After that some longitudinal reinforcement buckled at 4.5% drift at 0 to 250 mm high from the base of column and the damage continuously developed.

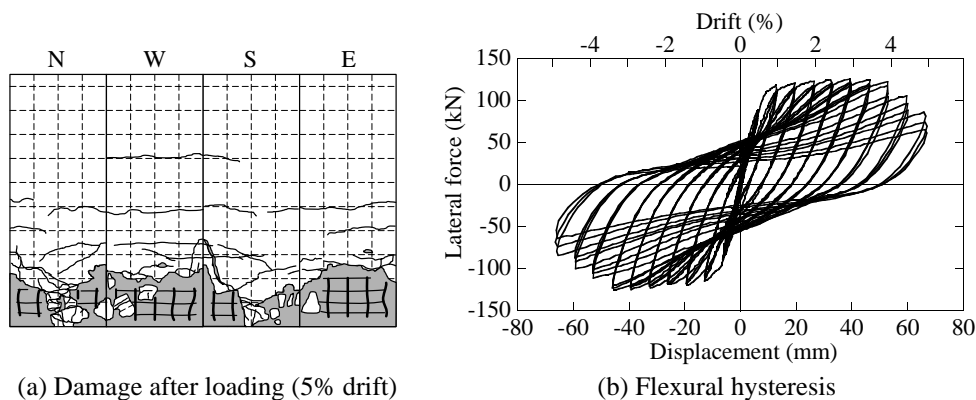


Fig. 5 Damage after testing and flexural hysteresis of column P1 (cyclic uniaxial bending with an axial force)

The flexural hysteresis of P1 is shown in Fig. 3(b). The column flexural restoring force is virtually stable between 1% to 4% drift with the flexural strength of 125.9 kN. The flexural restoring force starts to deteriorate at 3% drift because of the occurrence of compression failure in the covering concrete and the buckling of

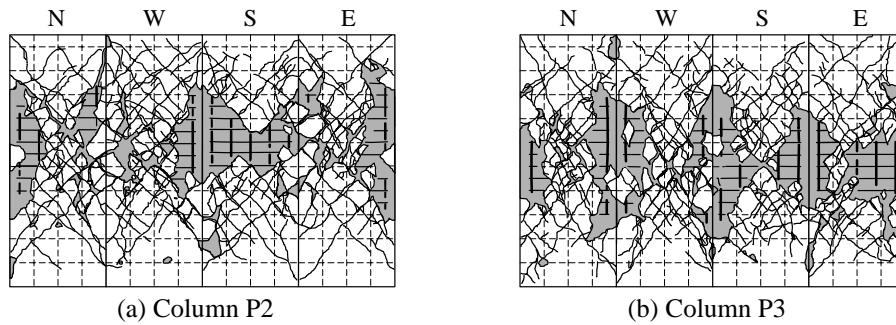


Fig. 6 Damage of columns P2 (cyclic torsion) and P3 (cyclic torsion with an axial force) at 0.09 rad rotation

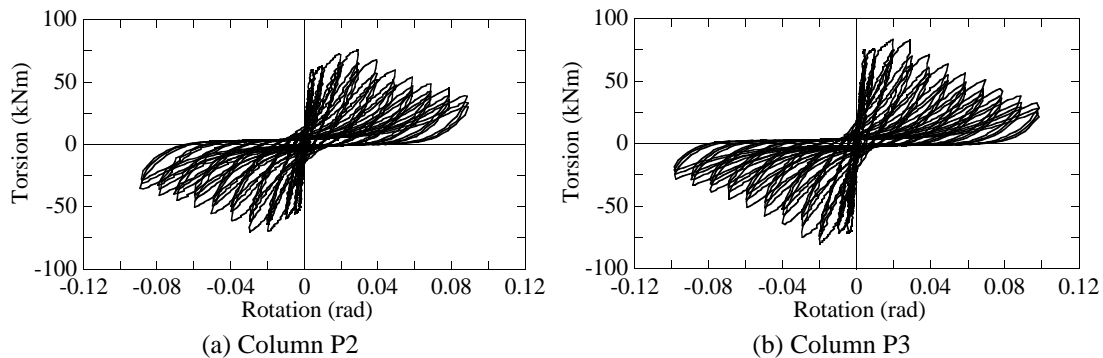


Fig. 7 Torsional hysteretic envelopes of columns P2 (cyclic torsion) and P3 (cyclic torsion with an axial force)

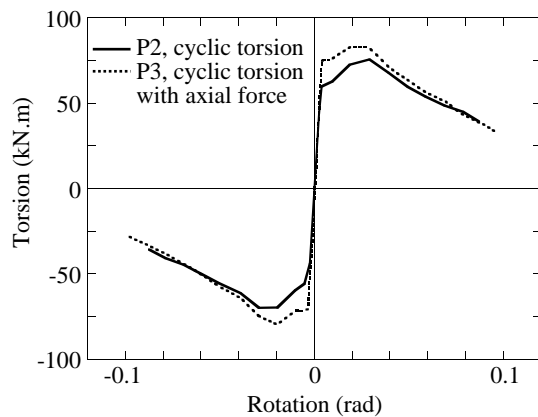


Fig. 8 Influence of axial force on torsional hysteretic envelopes.

longitudinal bars. Subsequently, the column loses the lateral confinement, and the flexural restoring force deteriorates to 68.7% of the flexural strength at 5% drift.

#### *Columns under Cyclic Torsion*

Diagonal cracks firstly initiated at 0.005 radian rotation cycle in both P2 and P3, which were subjected to cyclic torsion without and with the axial force, respectively. Subsequently, the number of cracks increased and the checker board crack patterns were developed on four column surfaces. Subsequently, the crack widths enlarged and the covering concrete of P2 and P3 spalled outward as the applied rotation increased. The damage of P2 and P3 at 0.09 radian is presented in Fig. 6. Finally, the significant damage occurred at the middle in both columns. The angles of cracks relative to the cross section of column were about 45 degrees in P2 while the larger angles of cracks were observed in P3. This is resulted from the effect of axial force. No buckling of longitudinal reinforcement was observed in P2 while the longitudinal bars slightly buckled outward in P3. The damage patterns of these two columns are significantly different to that of P1 under cyclic bending. Substantial damage occurred at the middle of column instead

of the typical flexural plastic hinge zone which is generally about a half of the column width from the base of column.

Fig. 7 compares the torsional hysteresses of P2 and P3. The torsional stiffness remarkably deteriorates after cracking at 0.005 radian rotation cycle in P2. The torsional strength reaches 75.7 kNm at 0.03 radian and it is followed by sharp deterioration due to the progress of damage at the middle of column. At 0.05 radian, the torsional capacity of P2 deteriorates to 78.8% of its strength. In P3, the torsional stiffness significantly deteriorates after cracking at 0.005 radian rotation cycle as in P2. Then P3 reaches the torsional strength of 83.4 kNm at 0.02 radian. The torsional strength of P3 is 10.2% larger and occurs earlier than P2. Then the torsional capacity of P3 progressively deteriorates to 76.3% of its strength at 0.05 radian. It is important to note that the effect of axial force becomes less significant as the rotation increases, based on the comparison of envelopes of P2 and P3 shown in Fig. 8. P2 and P3 fail in brittle manner compared to column P1 subjected to cyclic bending

### ***Column under Combined Cyclic Uniaxial Bending and Torsion***

Behavior of columns subjected to combined cyclic bending and torsion was investigated under four different rotation-drift ratios  $r$ . The damage at the end of loading on P4 to P7 is shown in Fig. 9. It can be seen that the S surface suffered more significant damage than the N surface. As described earlier, this was because the loading displacement resulted from combined bending and torsion was larger at the S surface than the N surface (refer to Figs. 2(b) and 3). Moreover, the angles of cracks relative to the column cross section increased as  $r$  increased. Compared to the damage of column subjected to cyclic bending in Fig. 5(a), more complex flexural and shear failure took place and the damage occurred outside the plastic hinge region as  $r$  increased. The damage pattern of P4 with  $r = 0.5$  is not much different from that of P1 which was subjected to pure cyclic bending. In contrast, the damage pattern of P7 with  $r = 4$  is close to that of P3 which was subjected to cyclic torsion with the axial force.

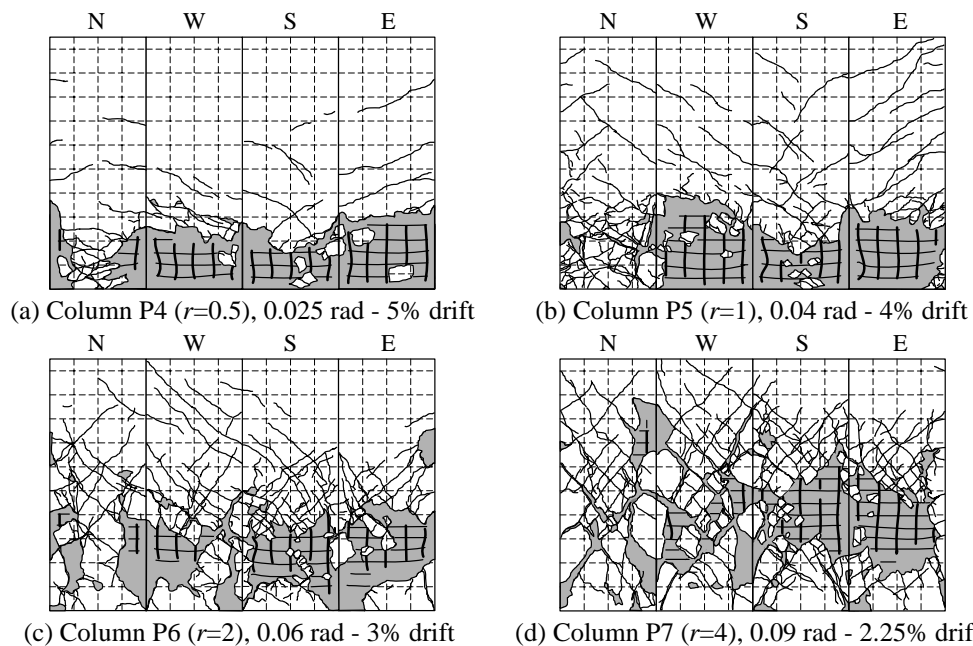


Fig. 9 Comparison of damage in columns P4 to P7 (combined cyclic bending-torsional loading) after testing

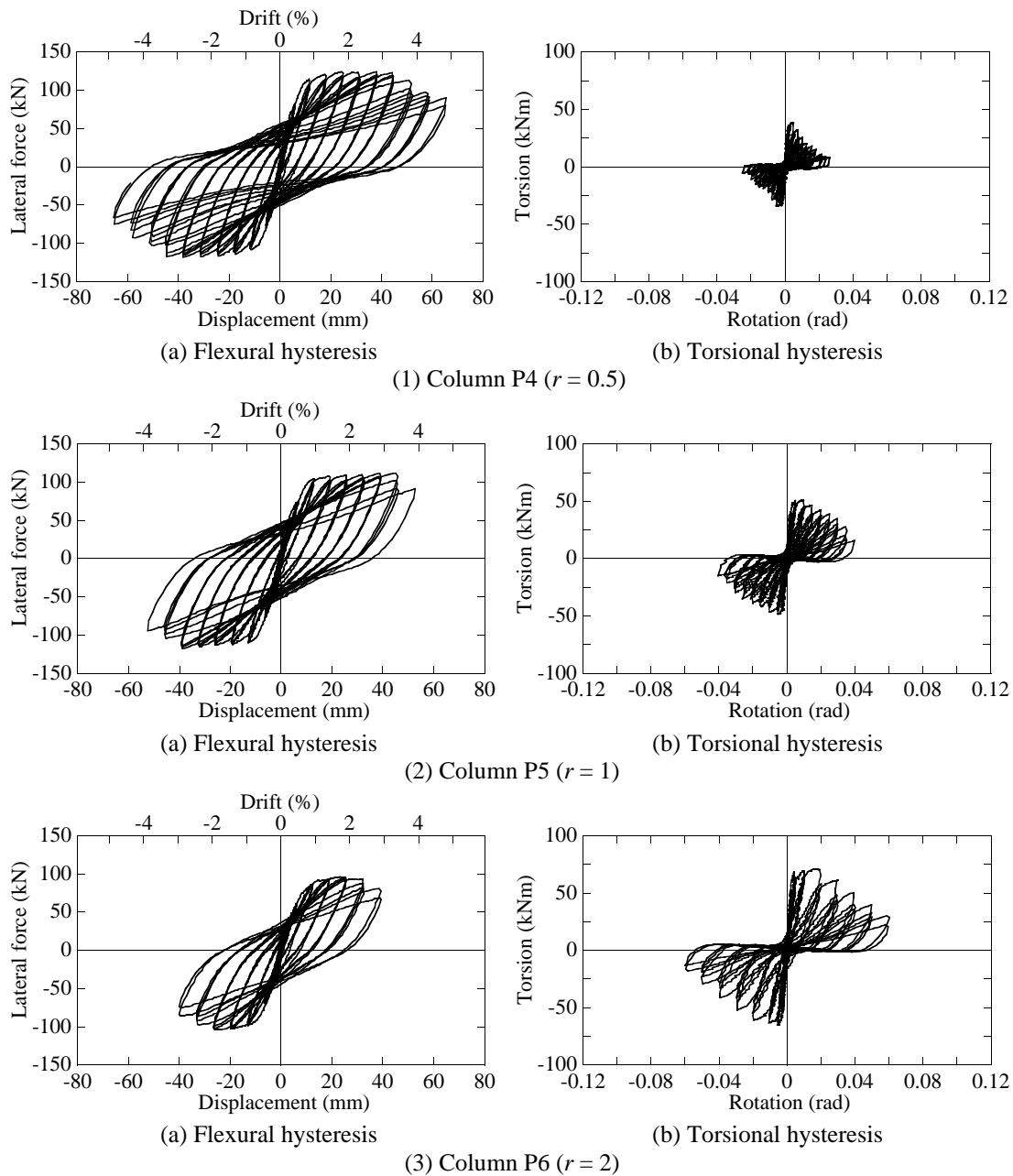


Fig. 10 Flexural and torsional hysteresses of columns under combined cyclic bending-torsional loading

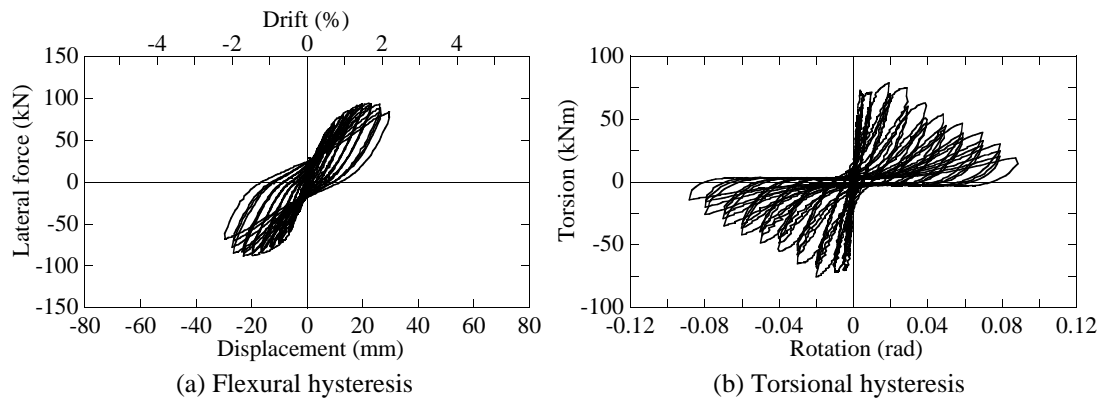
Fig. 10 shows the flexural and torsional hysteresses of P4 to P7. It can be observed that the flexural hysteresses of P5 to P7 under moderate to large  $r$  are significantly different to the flexural hysteresis of P1. It can be clearly seen that the flexural strength and the flexural ductility of columns decrease as  $r$  increases. On the other hand, the torsional strength and the torsional ductility increase as  $r$  increases.

### Effect of Combined Cyclic Uniaxial Bending and Torsion

#### *Strain in longitudinal and tie reinforcements*

Fig. 11 compares the strain hysteresses of longitudinal reinforcement at N-W





(4) Column P7 ( $r = 4$ )

Fig. 10 (Continued)

corner at 275 mm high from the bottom of column. The 275 mm level locates above the typical flexural plastic hinge region of the column. The yield strain of the longitudinal bars  $\varepsilon_{ly}$  of  $1717\mu$  is shown in Fig. 11. In P1, the longitudinal steel suffered the tensile strain when the column displaced to the positive side (E direction) and gradually changed to the compressive strain when the column moved to the negative side (W direction). The steel strain suddenly increased over  $2000\mu$  at 4% drift. In Figs. 11(b) to 11(e), significant difference of longitudinal bar strain can be observed as  $r$  increases. It is also noted that residual strains are much larger in the columns which are subjected to combined bending and torsion. However, the strain in longitudinal bar in P3 is much smaller than others. This may be attributed to the fact that damage shifts from the flexure plastic hinge region to the middle of columns as  $r$  increases.

Fig. 12 compares the strain hysteresses of tie reinforcement along S surface at 250 mm high from the column base. The  $1592\mu$  yield strain of tie reinforcement  $\varepsilon_{ty}$  is presented. The strain of tie reinforcement was small and it did not yield in P1. The strain of tie reinforcement increased as  $r$  increased. It is apparent that torsion results in larger deformation in the tie reinforcement. Similar to the above mentioned strain of longitudinal reinforcement, strain of tie reinforcement is not necessarily larger at P3 which was subjected to cyclic torsion. This may be attributed to the fact that the damaged zone shifts from the flexural plastic hinge zone to the middle of column as  $r$  increases.

### ***Envelopes of Hysteresses***

Fig.13 compares the envelopes of flexural and torsional hysteresses of columns. As explained earlier, the columns under cyclic torsion showed much brittle failure mode compared to the column under cyclic bending. Consistent variation of the strength and ductility are observed in both flexural and torsional hysteresses in accordance with the variation of  $r$ . It is noted that a stable lateral force zone in which lateral restoring force is nearly constant between 1% drift to 4% drift in the flexural hysteresses ( $r = 0$ ) is vanishing as  $r$  increases, resulted from softening of initial stiffness which is coupled with smaller flexural strength and earlier deterioration of lateral force. Consequently, not only deterioration of flexural strength but also deterioration of ductility capacity occurs as  $r$  increases. The flexural hysteretic envelope of column under the combined action becomes close to that of column under

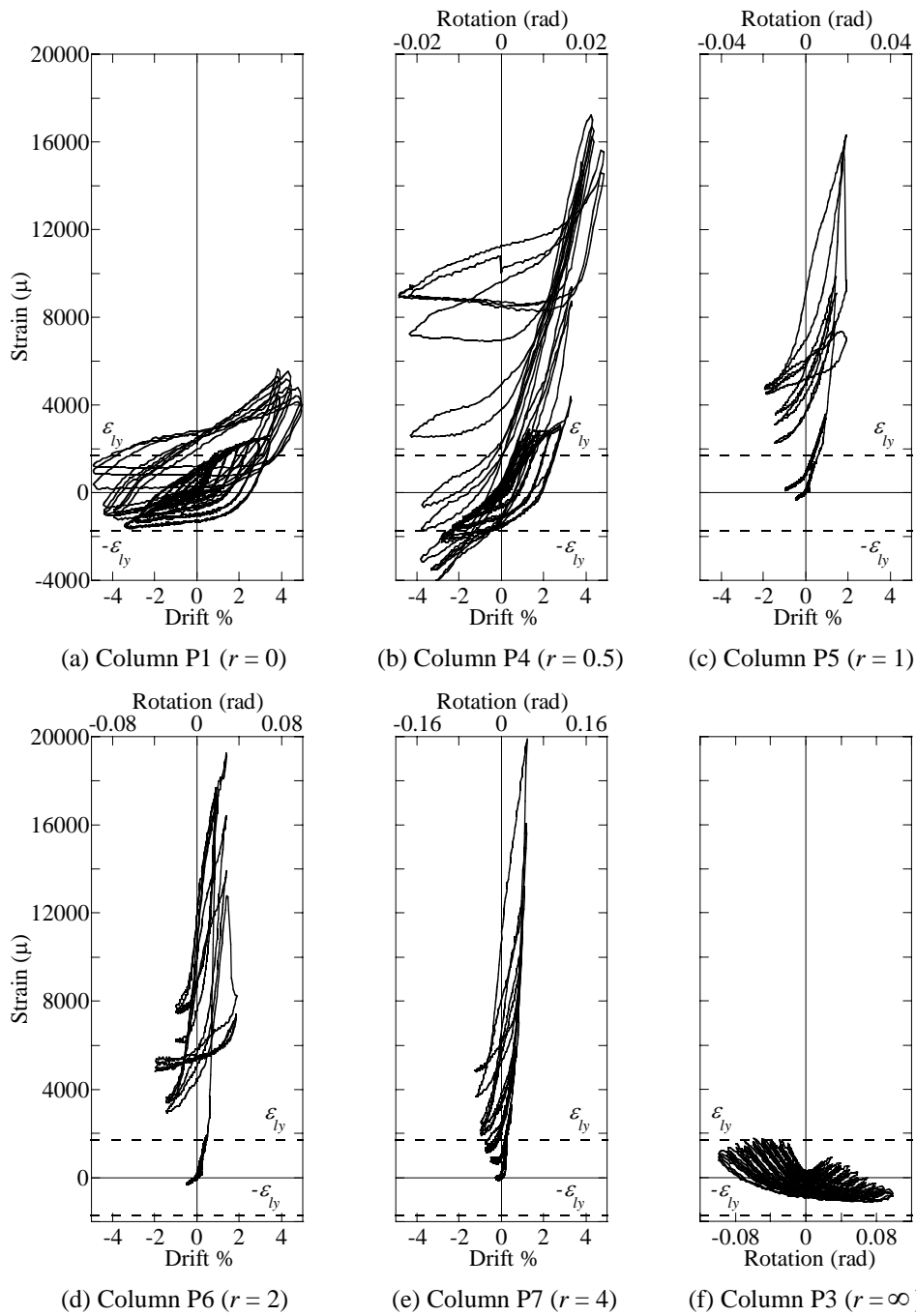


Fig. 11 Comparison of strain hystereses of longitudinal reinforcement at N-W corner at 275 mm high from the column base.

cyclic bending as  $r$  decreases.

On the other hand, in the torsional hystereses, torsion deteriorates immediately after taking peak value as  $r$  becomes less than 1. At  $r \geq 2$ , there exists a narrow zone in which torsion increases slightly or is almost flat with the increase of rotation. Consequently, care has to be paid for the brittle deterioration of torsional restoring force in a column which is subjected to cyclic torsion or combined action of cyclic torsion and cyclic bending. The hysteretic envelope under combined action becomes close to that under pure cyclic torsion with the axial force as  $r$  increases.

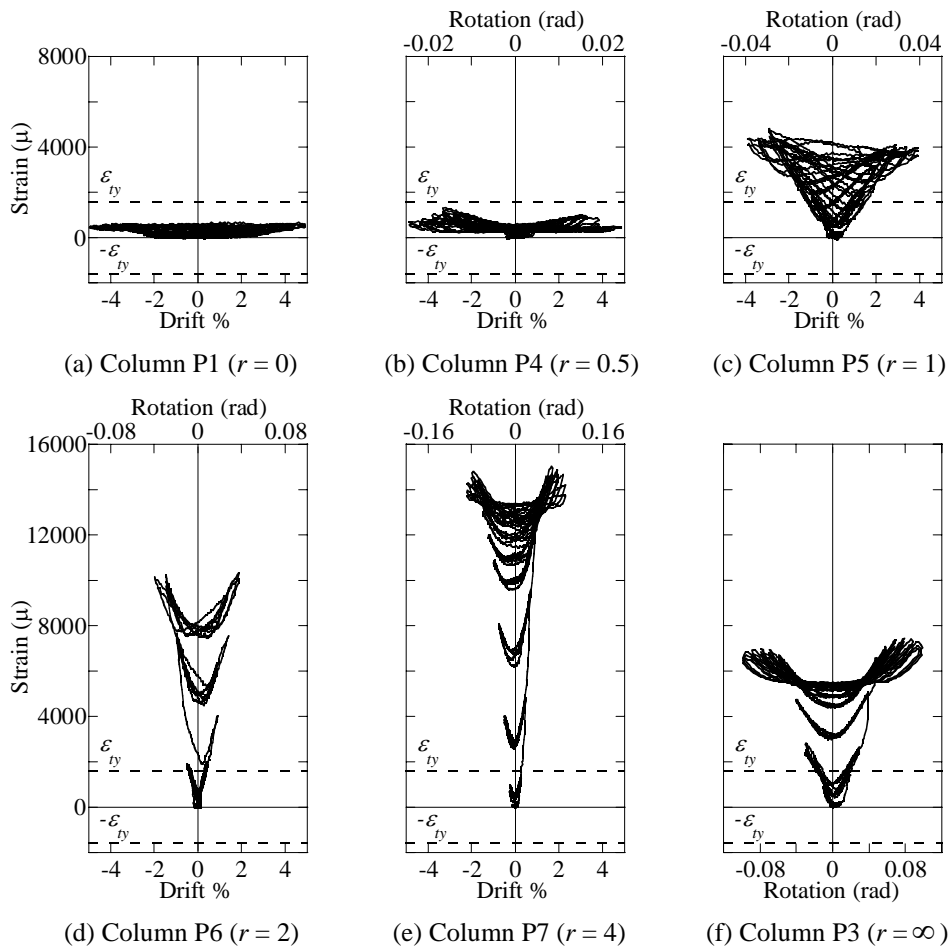


Fig. 12 Comparison of strain hysteresses of tie reinforcement on S surface at 250 mm high from the column base

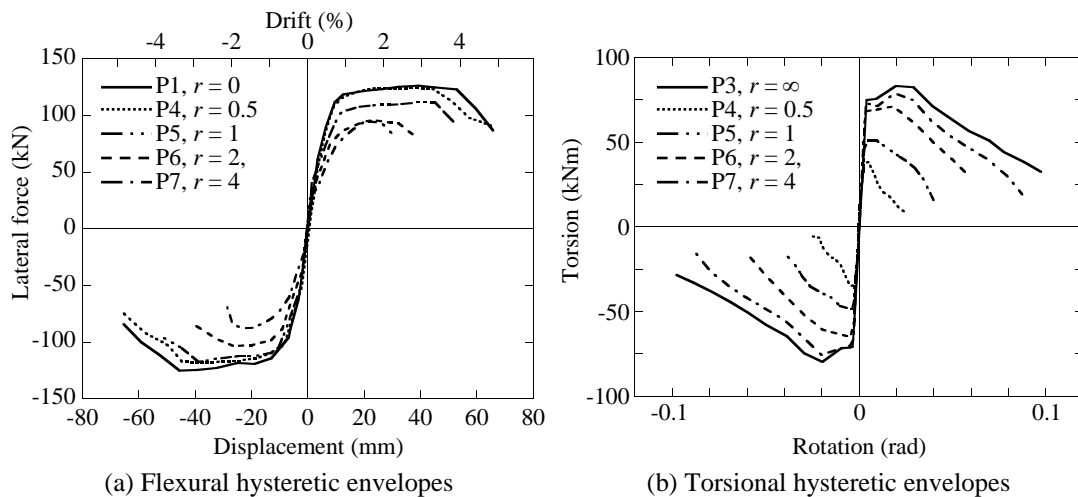


Fig. 13 Comparison of hysteretic envelopes of columns.

***Lateral force and torsional capacities, and ultimate displacement and rotation***

The maximum lateral force and torsional capacities, and the ultimate displacement and rotation of seven columns are summarized in Tables 3 and 4, respectively. The ultimate displacement is defined here as the displacement where the

Table 3 Maximum lateral forces and torsions

| Column | $r$      | Maximum lateral force (kN) |          |               | Maximum torsion (kNm) |          |              |
|--------|----------|----------------------------|----------|---------------|-----------------------|----------|--------------|
|        |          | Positive                   | Negative | Average       | Positive              | Negative | Average      |
| P1     | 0        | 125.9                      | 125.2    | 125.6 (100%)  | -                     | -        | -            |
| P2     | $\infty$ | -                          | -        | -             | 75.7                  | 70.0     | 72.9 (89.3%) |
| P3     | $\infty$ | -                          | -        | -             | 83.4                  | 79.7     | 81.6 (100%)  |
| P4     | 0.5      | 124.2                      | 118.5    | 121.4 (96.7%) | 38.4                  | 34.7     | 36.6 (44.8%) |
| P5     | 1        | 111.5                      | 117.9    | 114.7 (91.4%) | 50.8                  | 48.4     | 49.6 (60.8%) |
| P6     | 2        | 95.9                       | 103.8    | 99.9 (79.5%)  | 71.0                  | 64.9     | 68.0 (83.3%) |
| P7     | 4        | 94.4                       | 88.0     | 91.2 (72.6%)  | 79.0                  | 75.6     | 77.3 (94.8%) |

Table 4 Ultimate displacement and rotations

| Column | $r$      | Ultimate displacement (% drift) |          |              | Ultimate rotation (rad) |          |             |
|--------|----------|---------------------------------|----------|--------------|-------------------------|----------|-------------|
|        |          | Positive                        | Negative | Average      | Positive                | Negative | Average     |
| P1     | 0        | 5                               | 4.5      | 4.75 (100%)  | -                       | -        | -           |
| P2     | $\infty$ | -                               | -        | -            | 0.05                    | 0.05     | 0.05 (100%) |
| P3     | $\infty$ | -                               | -        | -            | 0.05                    | 0.05     | 0.05 (100%) |
| P4     | 0.5      | 4.5                             | 4.5      | 4.5 (94.7%)  | 0.01                    | 0.01     | 0.01 (20%)  |
| P5     | 1        | 4                               | 4        | 4 (84.2%)    | 0.025                   | 0.025    | 0.025 (50%) |
| P6     | 2        | 3                               | 3        | 3 (63.2%)    | 0.04                    | 0.04     | 0.04 (80%)  |
| P7     | 4        | 2.25                            | 2.25     | 2.25 (47.4%) | 0.04                    | 0.04     | 0.04 (80%)  |

lateral restoring force deteriorates to less than 80% of the flexural strength and the ultimate rotation is defined as the rotation where the torsional restoring force degrades to less than 80% of the torsional capacity. The results of P1 under cyclic uniaxial bending and P3 under cyclic torsion with the axial force are used as the benchmarks to evaluate the deterioration of the flexural and torsional strengths and the ultimate displacement and rotation of the columns under combined action. It is apparent that the flexural strength and the ultimate displacement deteriorate as  $r$  increases and the torsional strength and the ultimate rotation deteriorate as  $r$  decreases. At  $r = 4$ , the flexural strength and the ultimate displacement are 72.6% and 47.4% of the column under cyclic uniaxial bending, respectively. From P2 and P3, it is apparent that axial compression force enhances the torsional strength of column.

### Normalized Interaction Curves

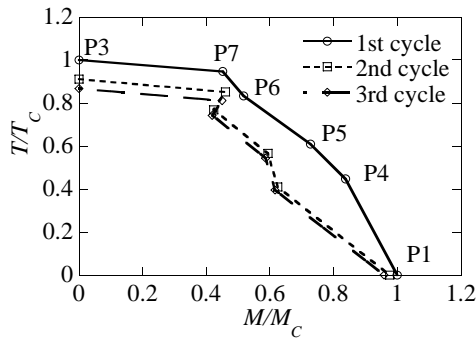


Fig. 14 Normalized interaction curves

Fig. 14 shows the normalized interaction curves between bending moment and torsion obtained from the experimental results. The value of each point in the plot is based on the maximum torsion or maximum bending moment, depending on which value the column reached first, and the corresponding bending moment or torsion. It is noted that the columns under combined cyclic bending and torsion reached their maximum torsions prior to the maximum bending moments. Torsion  $T$  of each

column is normalized by the maximum torsion  $T_c$  in the first loading cycle of P3 under cyclic torsion and bending moment  $M$  is normalized by the maximum bending moment  $M_c$  in the first loading cycle of P1 under cyclic bending. It can be seen that torsion deteriorates with the increase of the bending moment, and vice versa. The effect of number of loading cycles can also be observed from the difference between the curves of the first and second loading cycles. However, less significant difference is seen between the curves of the second and third loading cycles. This indicates that the deterioration of the column capacities is substantial in the first loading cycle and becomes less significant after columns undergo some more loading repetitions.

## Conclusions

An experimental study on the effect of combined cyclic uniaxial bending and torsion on the behavior of reinforced concrete columns was presented. Various combinations of bending and torsion in the form of the rotation-drift ratio  $r$  were tested to clarify the column performance. Based on the results presented herein, it may be concluded that:

- 1) Axial compression force enhances the torsional strength of column and enlarges the angle of cracks relative to the column cross section. However, the effect of axial compression force becomes less significant as the applied rotation increases after reaching the maximum torsion.
- 2) The existence of torsion alters the damage patterns of reinforced concrete columns under combined action. The complex flexural and shear failure tends to occur and the damage is likely to shift outside the typical flexural plastic hinge region to the middle of column as  $r$  increases. Because the length and location of plastic hinge significantly change, they have to be carefully evaluated in the column under combined bending moment and torsion.
- 3) The flexural capacity and the ultimate displacement of column deteriorate as the torsion increases. In contrast, the increase of bending moment leads to the deterioration of the torsional capacity and the ultimate rotation. Consequently, it is necessary to take account of this interaction in design of column subjected to the combined flexural and torsional load.
- 4) The relationship between the internal bending moment and torsion of columns can be performed as the normalized interaction curves. Increase of the number of loading cycles results in the reduction of the area enclosed by the interaction curve. However, the impact of number of loading cycles becomes less significant after columns experience more loading cycles.

## Acknowledgements

The authors express their sincere gratitude to Messrs. Watanabe, G., Fukuda, T., Nagai, T., Wang, Y., Ogimoto, H., Kijima, K., Nagata, S., Maruyama, Y. and Ms. Sakellaraki, D. for their extensive support in constructing the column specimens and executing the experiment.

## References

- 1) Hsu, H.-L. and Wang, C.-L., Flexural-Torsional Behavior of Steel Reinforced Concrete Members Subjected to Repeated Loading, *Earthquake Engineering and Structural Dynamics*, 29, 667–682, 2000.
- 2) Hsu, H.-L. and Liang, L.-L., Performance of Hollow Composite Members Subjected to Cyclic Eccentric loading, *Earthquake Engineering and Structural Dynamics*, 32, 433–461, 2003.
- 3) Japan Road Association, *Specifications for Highway Bridges - Part V Seismic Design*, Maruzen, Tokyo, 1996.
- 4) Kawashima, K., Watanabe, G., Hatada, S. and Hayakawa, R., Seismic Performance of C-bent Columns Based on a Cyclic Loading Test, *Journal of Structural Mechanics and Earthquake Engineering*, 745/I-65, pp.171–189, JSCE, 2003 (In Japanese)
- 5) Nagata, S., Kawashima, K. and Watanabe, G., Seismic Performance of Reinforced Concrete C-bent Columns Based on a Hybrid Loading Test, *Proc. of the First International Conference on Urban Earthquake Engineering*, Tokyo Institute of Technology, Tokyo, Japan, pp.409–416, 2004.
- 6) Otsuka, H., Wang, Y., Takata, T. and Yoshimura, T., Experimental Study on the Parameters Effecting the Hysteresis Loop of RC Members Subjected to Pure Torsion, *Journal of Structural Mechanics and Earthquake Engineering*, 739/V-60, pp.93–104, JSCE, 2003 (In Japanese)
- 7) Otsuka, H., Takeshita, E., Yabuki, W., Wang, Y., Yoshimura, T. and Tsunomoto, M., Study on the Seismic Performance of Reinforced Concrete Columns Subjected to Torsional Moment, Bending Moment and Axial Force, *13th World Conference on Earthquake Engineering*, Vancouver, Canada, Paper No. 393, 2004
- 8) Tirasit, P. and Kawashima, K., Seismic Torsion Response of Skewed Bridge Piers, *Journal of Earthquake Engineering*, 28, Paper No. 116, 2005.
- 9) Watanabe, G. and Kawashima, K., Effectiveness of Cable-restrainer for Mitigating Rotation of a Skewed Bridge Subjected to Strong Ground Shaking, *13th World Conference on Earthquake Engineering*, Vancouver, Canada, Paper No. 789, 2004.